Calculation of the Track Width of Ropeways

G. Oplatka and M. Volmer[1]

1 Introduction

The track width of a ropeway is defined as the distance between the tracks that carry the cabins. In some installations the tracks may not be parallel to each other. This is often so in jig-back tramways. In this case the track width will not be constant over the track length. Figure 1 is a sketch of the features of a jig-back tramway and illustrates the definition of the track width and other terms.

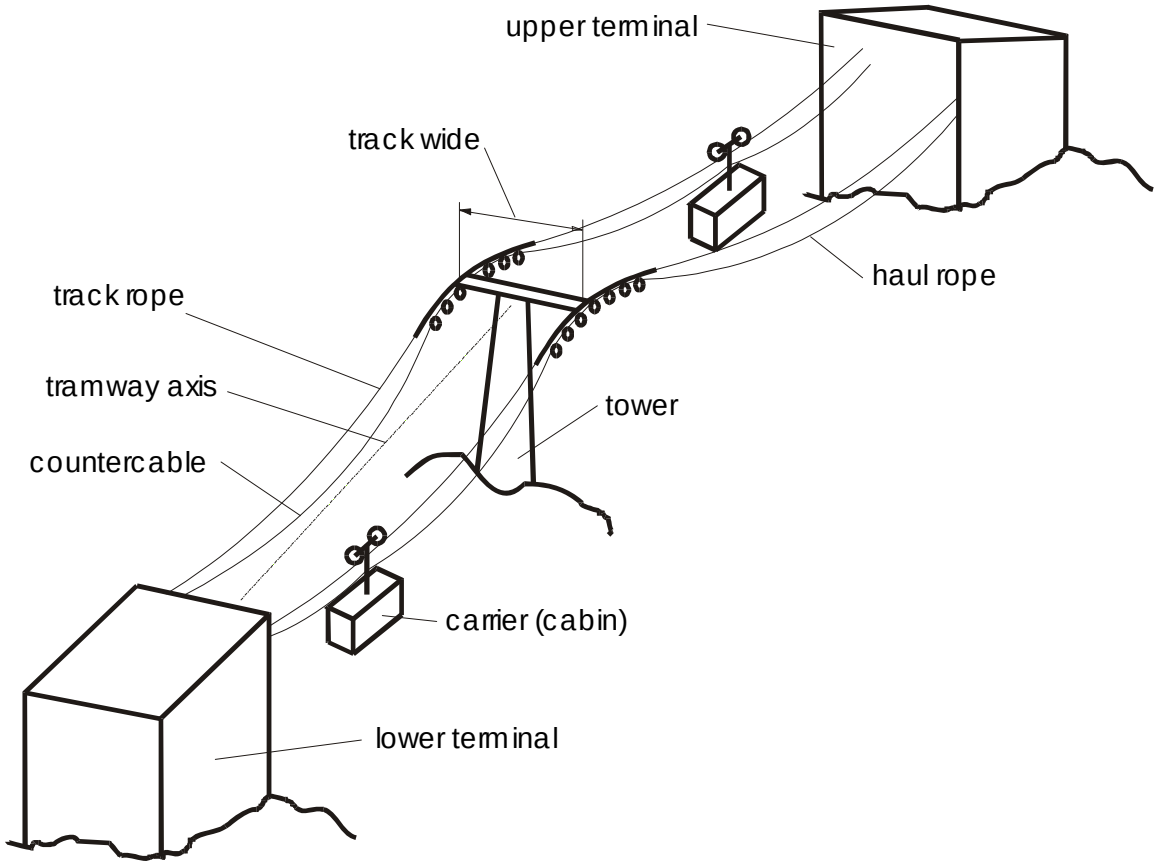

[1] The authors Prof.dr. dr. h.c. Gabor Oplatka and M. Volmer are members of the Institute of Lightweight Structures and Ropeways of the Swiss Federal Institute of Technology (ETHZ) Zürich

ETH Zentrum LEO / ILS
Leonhardstrasse 27
CH – 8092 Zürich
Phone: +41 1 633 32 51
Fax: +41 1 633 11 10
Email: volmer@ils.mavt.ethz.ch

Figure 1. Definition of the track width of a jig-back tramway
The track width of other ropeways, such as continuously circulating ones is defined analogously.

The upward and downward travelling cabins pass by in double track jig-back ropeways and in continuously circulating ones. Cabins experiencing a side-wind will be displaced in the direction of the wind. This may cause the distance between the cabins travelling in opposite directions to decrease, even to the extent that a collision may occur. The probability of such an accident must be kept within reasonable limits by keeping the tracks far enough apart or by other means. Thus the cabins may be streamlined, guides at the towers may be provided and other provisions may be made at the design stage.

With increased track width the length of the cross girders on the towers and the size of the terminals increase as does the cost of the whole installation. One tries therefore to keep the track width as small as possible. For safety on the other hand the track width must be large enough to avoid the danger of collision and that of deropement at the towers.

1.2 Definition of the problem

Up to now the track widths of jig-back tramways and continuously circulating ropeways were calculated according to heuristic formulas prescribed in Switzerland by the Swiss Federal Traffic Authority (BAV – Bundesamt für Verkehr), based on the work of Prof.Bittner of Vienna, Austria. The application of these formulas to large track widths and new types of ropeways (such as Funitel, 3S) has been questioned. Also the physical modelling of these formulas is insufficient.

To judge the characteristics of a rope span pair and to estimate the probability of two ropes touching or even cabins carried on the ropes colliding, two areas have to be considered. These are:

- the behavior of the rope span under dynamic wind load. Both the spacial distribution of the wind velocity and its behavior in time are important.

- the effect of the dynamic pressure on the cabins.

The smallest effective width of the track will depend on the maximum expected displacement of the rope span (possibly with a shift of phase) and the clearance gauge of the cabins. Rope displacements are caused by gusts of side-wind. The pressure distribution on rope spans caused by such winds is still unknown. This is especially true for long spans. An additional difficulty is that the resulting modes of oscillation have not been studied sufficiently.

1.3 Aim of this study

In this study we aim to define a method to determine track width of a ropeway as a function of the type of ropeway, the meteorological conditions (especially wind), the different loading conditions and the longitudinal profile. These values must be found at a confidence level that allows to quantify the probability of collision of two cabins travelling in opposite directions.

2 The wind model

To find the system behavior of a ropeway a suitable modelling of the wind forces is important. The Reynold numbers that occur in the air flow pattern around ropeways indicate clearly that the flow is turbulent. The flow pattern can be defined in the direction of its height somewhat more exactly by defining a boundary layer region and a gradient region.

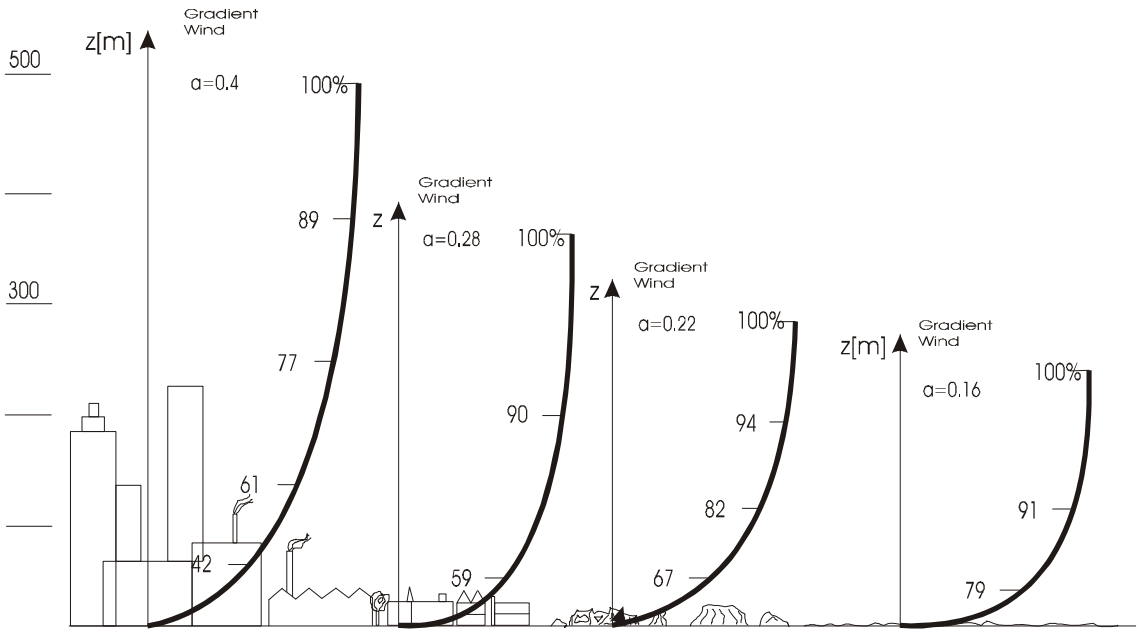

Figure 2. Wind profiles for medium wind velocity blowing over ground with different degrees of roughness [1]

The velocity characteristic on the left may be taken to apply in the typically rough ground of the mountains. The thickness of the boundary layer is therefore about 500 meters, that is, ropeways experience an air current in the boundary layer region. It should be noted that the flow in the boundary layer is mostly stochastic. Methods of probability theory were therefor used to describe the flow velocity [2]. This has the advantage that stochastic processes can be described as such. They have the disadvantage on the other hand that they are purely descriptive and they do not help to explain the physical process leading to turbulence.

The wind velocity at a specific point in the air flow pattern is generally characterized (for instance in [3]) by its power spectrum. Normalizing this spectrum with the variance of

the wind velocity and its frequency gives a relative spectrum of the wind velocity that is a dimensionless quantity. To a good approximation this quantity is the same at all points of the flow pattern. The most famous example of this is the Davenport spectrum, as follows:

$$\frac{f \cdot S_{uu}(f)}{\sigma^2} = \frac{2}{3} \frac{x_1^2}{(1+x_1^2)^{4/3}} \tag{1}$$

where x_1

$$x_1 = \frac{L}{\bar{u}(10)} f \tag{2}$$

represents a dimensionless frequency. Besides (1) other spectra are used, such those called after Harris, Hino, Simiu and Kaimal. They each give more or less differing values that, differ also from measured ones. These differences can affect the accuracy of calculating track width. Figure 3 gives a comparison of most of the spectra used today.

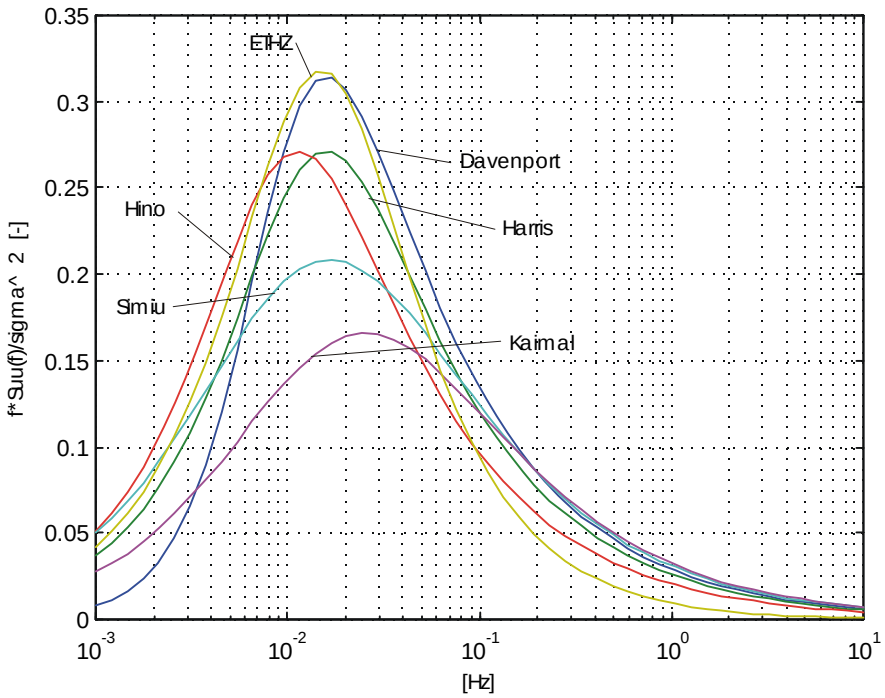

Figure 3. Comparison of wind power spectra used today

Equation (1) defines the excitation of the ropeway as a system so to say completely. Yet it is clearly the air velocity differs at different points along the rope span. In other words we are looking for a function that describes the effect of the wind on the rope as a function of structural dimensions. In other words this function describes the air stream

at its various points. The air stream itself is defined mainly by the strength of the wind gust.

We can imagine of the turbulent air flow consisting of both: the wind and the gusts. The latter have a velocity patterns around the median, while they all are in the range of medium wind velocities $\bar{u}$. Figure 4 shows this model.

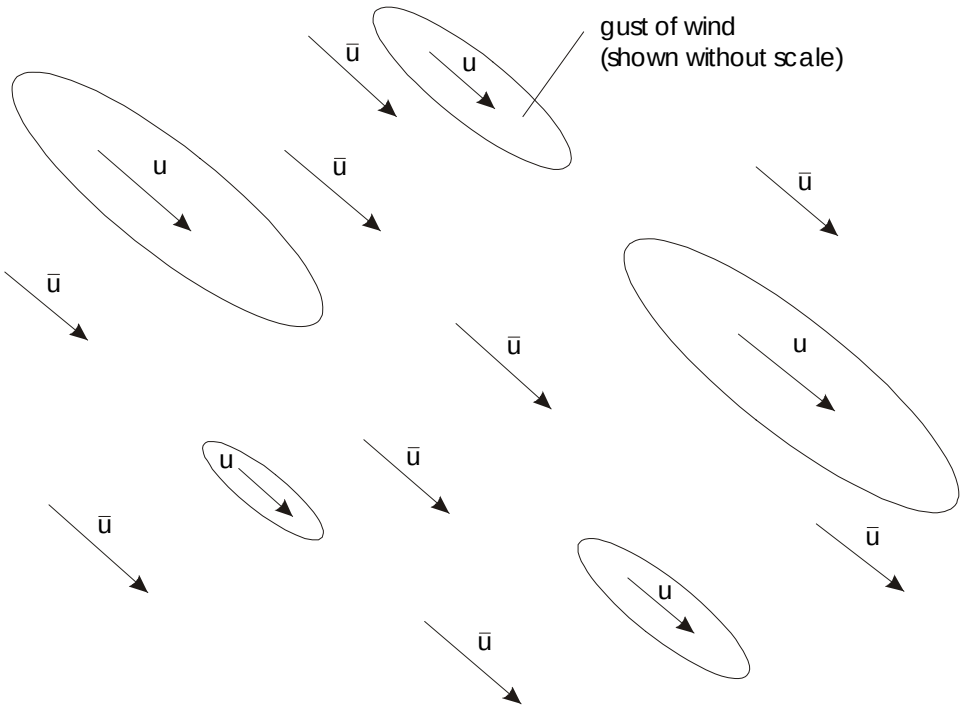

Figure 4. Turbulence structure

The ellipses of Figure 4 represent the size of a gust of wind. This is defined by

$$L_p = \int_0^{\infty} \rho_{uu}(x) \cdot dx \qquad (3)$$

Here $\rho_{uu}(x)$ is the relative spatial autocorrelation function of the air flow pattern. Using this definition of the size of the gust and considering typical dimensions of ropeway structures it is possible to calculate the so called aerodynamic transfer function of a large size rope with sag, as follows:

$$\left|A(f)\right|^2 = \frac{4 \cdot \overline{M}^2}{(c \cdot k \cdot f)^2 + \bar{u}^2} \qquad (4)$$

$\overline{M}$ is the momentum applied to the rope span by the median wind velocity, *c* is the rope chord of the rope span, $\bar{u}$ is the median wind velocity, *k* is a factor that depends on the size of the wind gust and should be measured in the field.

It should be emphasized that equation (4) is valid for a large size rope with sag. A ropeway installation includes also elements with a cuboid geometry, that is, cabins. Another aerodynamic transfer function, called after Vickery [4] is used for these ones. It is as follows:

$$|A(f)|^2 = \frac{4 \cdot \overline{F}}{\overline{u}} \frac{1}{1+\left[\frac{2f \cdot \sqrt{A}}{\overline{u}}\right]^{4/3}} \qquad (5)$$

Here *A* is the surface area of the side of the cabin, $\overline{F}$ is the force on the side of the cabin caused by the median wind velocity $\overline{u}$. There are other aerodynamic transfer functions in use, among others those of Davenport and Ruscheweyh [5]. They describe the forces on cubic structures and also high rectangular ones, such as towers and chimneys. Figure 5 gives a comparison among aerodynamic transfer functions.

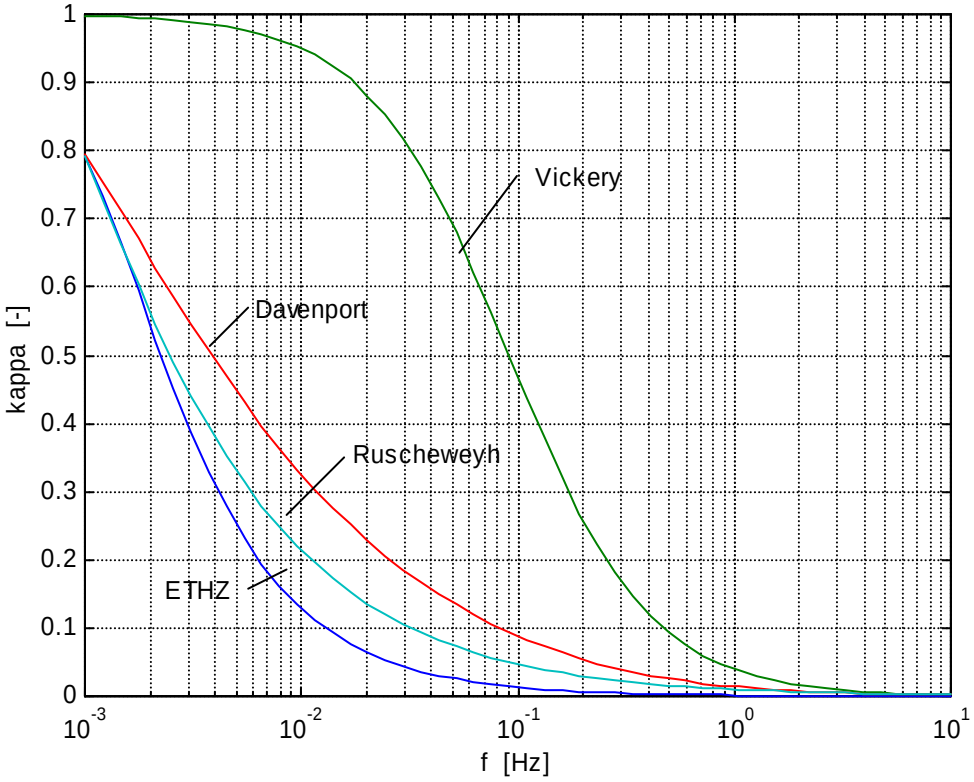

Figure 5 A comparison of aerodynamic transfer functions

3 Modelling the ropeway

The behavior of the ropeway has still to be described. A rope span can oscillate in two mutually perpendicular directions. Changes in the rope travel velocity due to the drive of the ropeway, such as emergency braking cause longitudinal oscillations and ones in the vertical plane (transverse oscillations). Only transverse oscillations in the direction of the y-axis of Figure 6 affect the dimensioning of the track width.

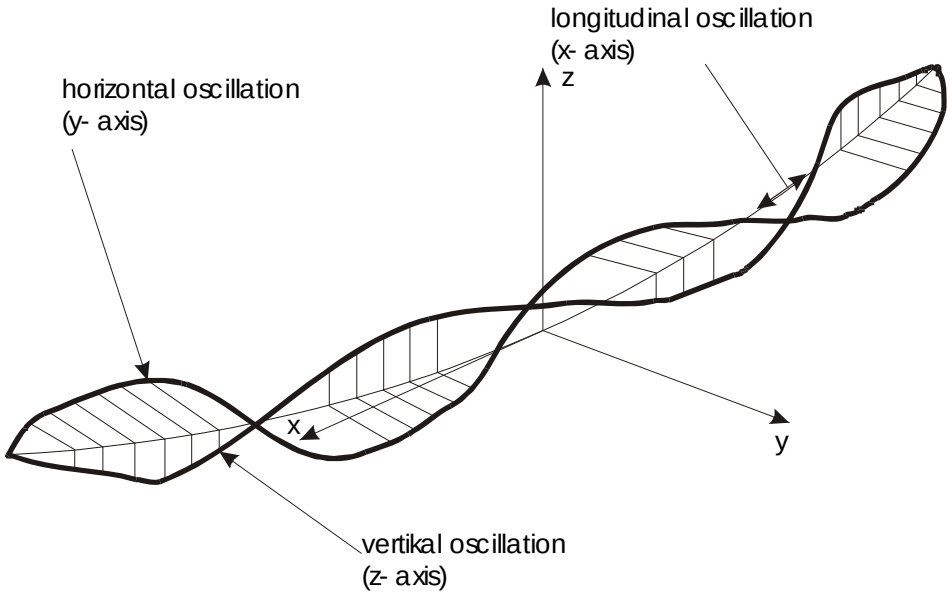

Figure 6. Directions of oscillation of the rope span

A more profound mathematical analysis of the oscillations in a rope span with sag shows that the swinging of the rope span around the rope chord (*c*) is mechanically decoupled both from the transverse waves along the z-axis and from the longitudinal waves along the x-axis. The wind cannot cause higher frequency oscillations (higher modes) in rope spans as shown in Figure 6 because the spectrum of the exciting forces (see Section 4) is too narrow. Therefore the rope span may be regarded as a swinging oscillator with several degrees of freedom. The first of these is that of the rope span itself, others may be allocated to cabins placed in it. Figure 7 shows a possible configuration with three cabins in span.

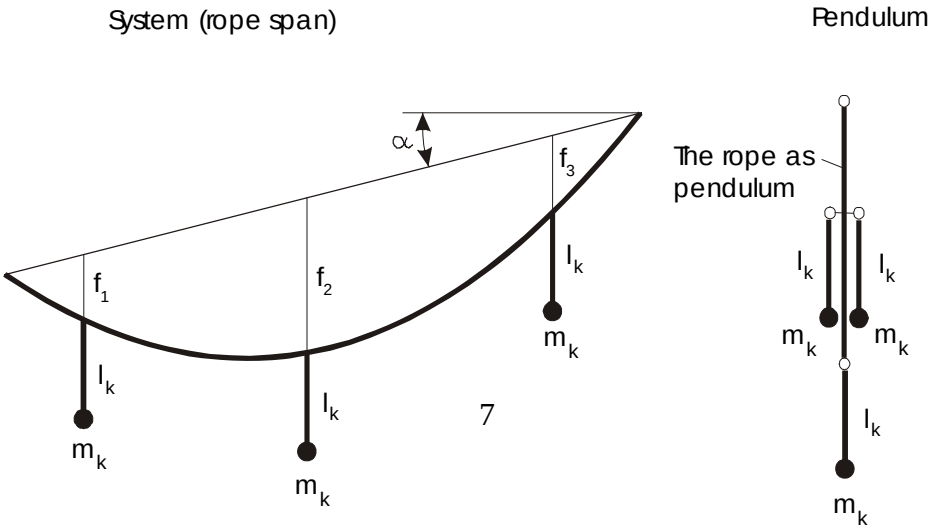

Figure 7. Model of a rope span with three cabins as a four mass pendulum

Note that Figure 7 shows a standing still ropeway, that is, with zero travelling speed. This simplification is permissible because we consider only low frequency oscillations in the rope span. The general equation of movement of the ropeway as a mechanical system is as follows:

$$\underline{\underline{M}} \cdot \underline{\ddot{\varphi}} + \underline{\underline{D}} \cdot \underline{\dot{\varphi}} + \underline{\underline{K}} \cdot \underline{\varphi} = \underline{m}(t) \qquad (6)$$

Here $\underline{\underline{M}}$ is the matrix of the masses, $\underline{\underline{D}}$ represents the damping, $\underline{\underline{K}}$ is the matrix for stiffness of the mechanical system, $\underline{\varphi}$ represents the pendulum vector of the angle of the displaced system shown in Figure 8 and $\underline{m}(t)$ is the excitation by the side wind as a function of time.

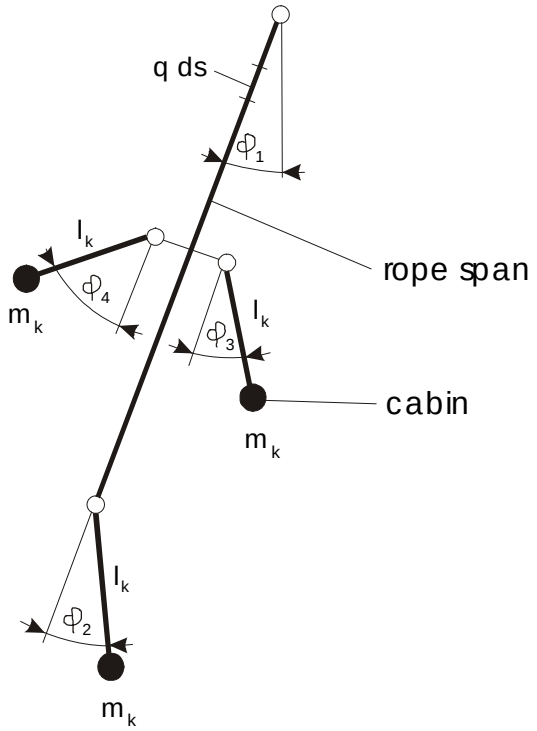

Figure 8. Pendulum system of Figure 7 shown angularly displaced

It is difficult to apply equation (6) because the damping factor $\underline{\underline{D}}$ is usually unknown, while damping has a substantial influence on the displacement of the system. The reason for this is that according equation (6) a force with a continuous frequency spectrum excites the system. Excitation will take place at resonance frequencies of (6) therefore, and the system response will be highly dependent on the damping $\underline{\underline{D}}$. The value of this, or at least of some of its components, is estimated in measurements carried out on an existing Funitel installation (refer to Section 6).

Performing a Fourier transformation on equation (6) results in the frequency dependent magnification function $\underline{\underline{G}}(f)$ of the ropeway as a mechanical system. It describes completely the frequency dependent transfer behaviour of the installation as follows:

$$\underline{\underline{G}}(f) = \left[-4\pi^2 f^2 \cdot \underline{\underline{M}} + 2\pi i f \cdot \underline{\underline{D}} + \underline{\underline{K}}\right]^{-1} \qquad (7)$$

4 Amplitude spectrum

Up to now we dealt separately with the definition of the problem of wind spectra and with the transfer functions wind - ropeway on the one hand and the mechanical behavior of the ropeway on the other. In this section we shall combine these using the tools of system theory.

The exiting by side wind is a stochastic process and can therefore be described conveniently as a range of frequency. Because all partial problems as the power spectrum of the wind, and the aerodynamic and mechanical transfer functions of the ropeway are already known, we can therefore combine these as follows, using system theory:

$$\underline{\underline{S}}_{\varphi\varphi}(f) = \underline{\underline{G}}(f) \cdot \underline{\underline{A}}(f) \cdot \underline{\underline{S}}_{uu}(f) \cdot \underline{\underline{A}}^{*}(f) \cdot \underline{\underline{G}}^{*}(f) \qquad (9)$$

Here $\underline{\underline{S}}_{\varphi\varphi}(f)$ is the amplitude spectrum of the system response, and $\underline{\underline{G}}(f)$, $\underline{\underline{A}}(f)$ and $\underline{\underline{S}}_{uu}(f)$ are the functions described in section 2 and 3. Equation (9) is displayed commutatively as follows:

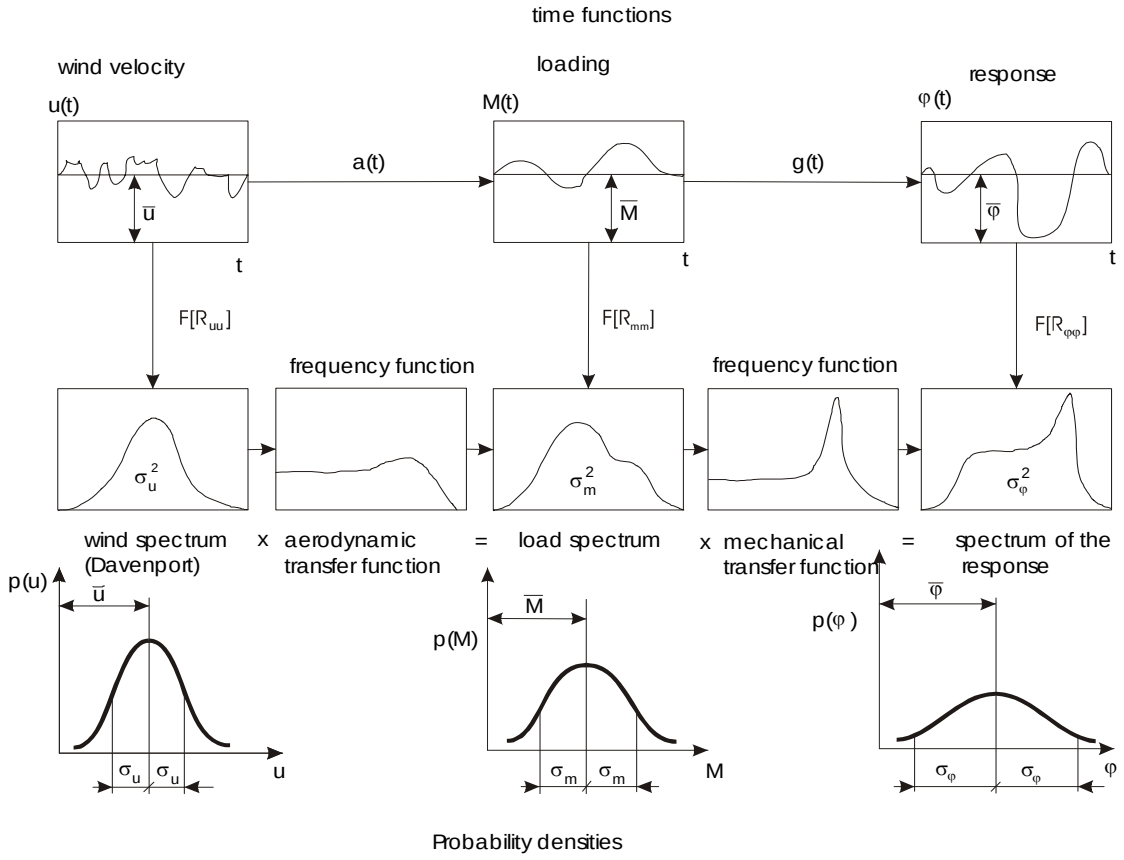

Figure 9. Schematic illustration of the calculation of the response spectrum

To calculate the track width we shall use the amplitude of the oscillations. Its variance, from equation (9), is as follows:

$$\underline{\underline{C}}_{\varphi\varphi} = \int_{-\infty}^{\infty} \underline{\underline{G}}(f) \cdot \underline{\underline{A}}(f) \cdot \underline{\underline{S}}_{uu}(f) \cdot \underline{\underline{A}}^{*}(f) \cdot \underline{\underline{G}}^{*}(f) \cdot df \qquad (10)$$

Note that $\underline{\underline{C}}_{\varphi\varphi}$ is a matrix whose elements are the variances and covariances of the response process. It has the following internal structure:

$$\underline{\underline{C}}_{\varphi\varphi} = \begin{bmatrix} \sigma_1^2 & C_{12} & \cdot & \cdot & C_{1i} & \cdot & \cdot & C_{1n} \\ C_{12} & \sigma_2^2 & \cdot & \cdot & \cdot & \cdot & \cdot & \cdot \\ \cdot & \cdot & \cdot & \cdot & \cdot & \cdot & \cdot & \cdot \\ \cdot & \cdot & \cdot & \cdot & \cdot & \cdot & \cdot & \cdot \\ C_{1i} & \cdot & \cdot & \cdot & \sigma_i^2 & \cdot & \cdot & \cdot \\ \cdot & \cdot & \cdot & \cdot & \cdot & \cdot & \cdot & \cdot \\ \cdot & \cdot & \cdot & \cdot & \cdot & \cdot & \cdot & \cdot \\ C_{1n} & \cdot & \cdot & \cdot & \cdot & \cdot & \cdot & \sigma_n^2 \end{bmatrix} \qquad (11)$$

5 Track width

The characterization of the process in Section 4 allows us to calculate the track width of the ropeway. To do this we have to propose the track width as defined spacing. There are some ways to do this. Here we shall regard track width as a state variable as illustrated in Figure 10.

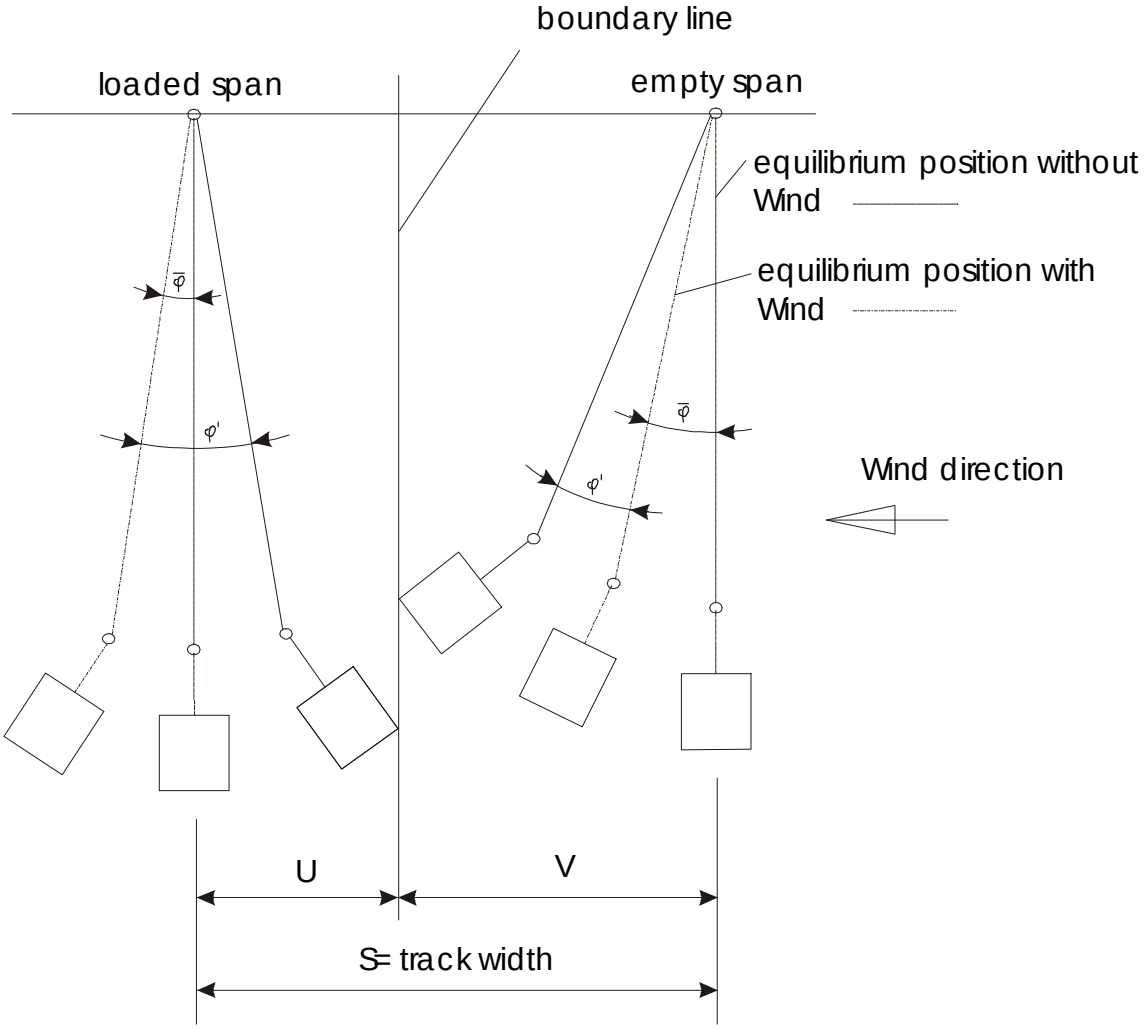

Figure 10. Definition of track width *S* in free span

The track width is the sum of the two partial lengths *U* and *V*. These are the probability rates of the maximum displacement of the upward and downward traveling cabins. The track width *S* is therefore defined as

$$S = U + V \tag{12}$$

Each quantity *S, U,* and *V* consists of its median $\overline{S}$, $\overline{U}$, and $\overline{V}$ and a time dependent function *S', U'* and *V'* .

Because usually the upward travelling cabins are not equally loaded as the downward travelling ones, the sags of the corresponding span are different too. Presupposing sufficient difference in the loads of the cabins by strong, gusty wind one could therefore imagine a situation shown in Figure 11. Here cabins travelling in the two directions pass under (or over) each other without colliding.

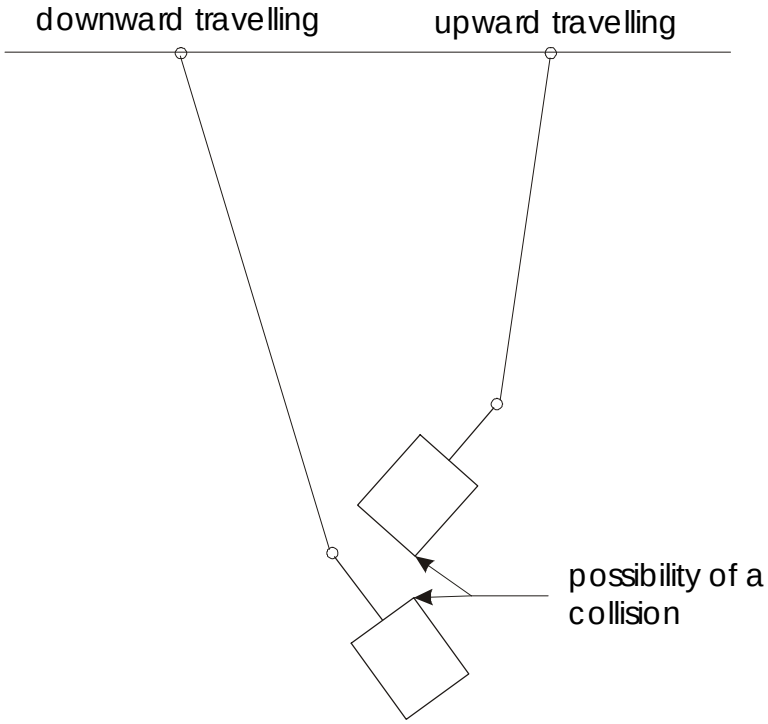

Figure 11. Cabins passing under each other without colliding

In the operational situation of Figure 11 problems may arise on a change in speed of the installation as occurs on an emergency stop for instance. Then the rope spans oscillate with comparatively large amplitudes in the vertical plane that may cause a collision of the cabins. Because it must be possible to stop a ropeway in any operational situation, cross-over of the two tracks is therefore not permissible. This is indicated in Figure 10.

We regard the quantities *U, V, S* defined in Figure 10 as random variables characterized by probability density. The wind velocity *u,* itself a random variable, has an amplitude distribution that is normal (Gaussian) as shown by measurements and by the limit value theorem [1], [7]. Figure 12 shows this distribution.

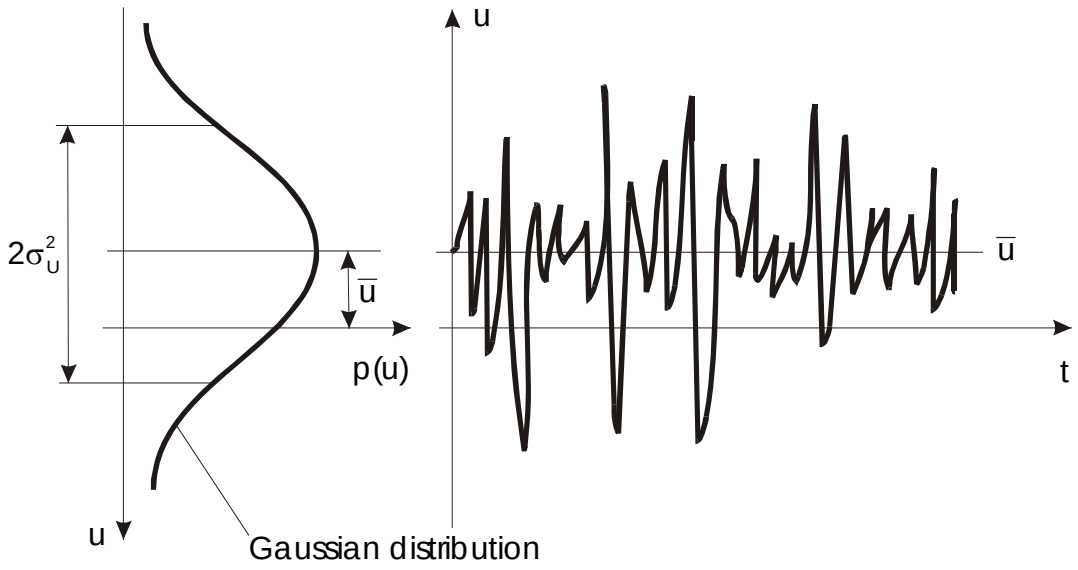

Figure 12 Amplitude distribution density of wind velocity

It can be shown that the type of distribution density of the input function is conserved in linear transfer systems, as considered in Section 4. This means that the distribution density of the amplitude of oscillations in the rope span considered must be Gaussian. The Gaussian distribution is particularly convenient to use in calculations as it is fully characterized by its median (expectation) and the variance of the process it represents. Both the median and the variance of the process we considered have been calculated.

The variance (11) has been constrained to the degrees of freedom that are of interest here. We need to consider only the influence of those cabins at midspan of continuously circulating ropeways and those at the passing point in jig-back tramways. The influence of cabins outside these positions may be neglected. The multivariable probability densities indicated in Figure 10 may be reduced therefore to the elements shown within the frame in (12). Note that the numbering of the matrix elements may not correspond to the degrees of freedom of the mechanical system.

$$\underline{\underline{C}}_{\varphi\varphi} = \begin{bmatrix} \sigma_1^2 & C_{12} & \cdot & \cdot & C_{1i} & \cdot & \cdot & C_{1n} \\ C_{12} & \sigma_2^2 & \cdot & \cdot & \cdot & \cdot & \cdot & \cdot \\ \cdot & \cdot & \cdot & \cdot & \cdot & \cdot & \cdot & \cdot \\ \cdot & \cdot & \cdot & \cdot & \cdot & \cdot & \cdot & \cdot \\ C_{1i} & \cdot & \cdot & \cdot & \sigma_i^2 & \cdot & \cdot & \cdot \\ \cdot & \cdot & \cdot & \cdot & \cdot & \cdot & \cdot & \cdot \\ \cdot & \cdot & \cdot & \cdot & \cdot & \cdot & \cdot & \cdot \\ C_{1n} & \cdot & \cdot & \cdot & \cdot & \cdot & \cdot & \sigma_n^2 \end{bmatrix} \qquad (13)$$

This allows us to describe completely the compound distribution except of the angle of dislocation $\underline{\varphi}$, whose median is considered separately.

$$P(\underline{\varphi}) = \frac{1}{\sqrt{(2\pi)^n \det \underline{\underline{C}}_{\varphi}}} \cdot e^{-\frac{1}{2}\cdot \underline{\varphi}^T \underline{\underline{C}}_{\varphi}^{-1} \cdot \underline{\varphi}} \qquad (14)$$

This does not yet define the track width *S* or its components *U* and *V* (Figure 10) because (14) is dealing only with distribution of displacement angle. The distribution densities for *U* and *V* are calculated with the help of (14) from the distributions for the upward and downward travelling sections of carrying rope. The behaviour of (14) obtained for the ropes travelling in the two directions will, of course, normally differ as the track loadings are different. The expression (14) is suitable to transform the random variables *U* and *V*. Next step will be used to transform distribution densities of *U* and *V* to transform them into distribution density of track width *S*, because it is a random variable itself. The mathematical procedure is illustrated schematically in Figure 13.

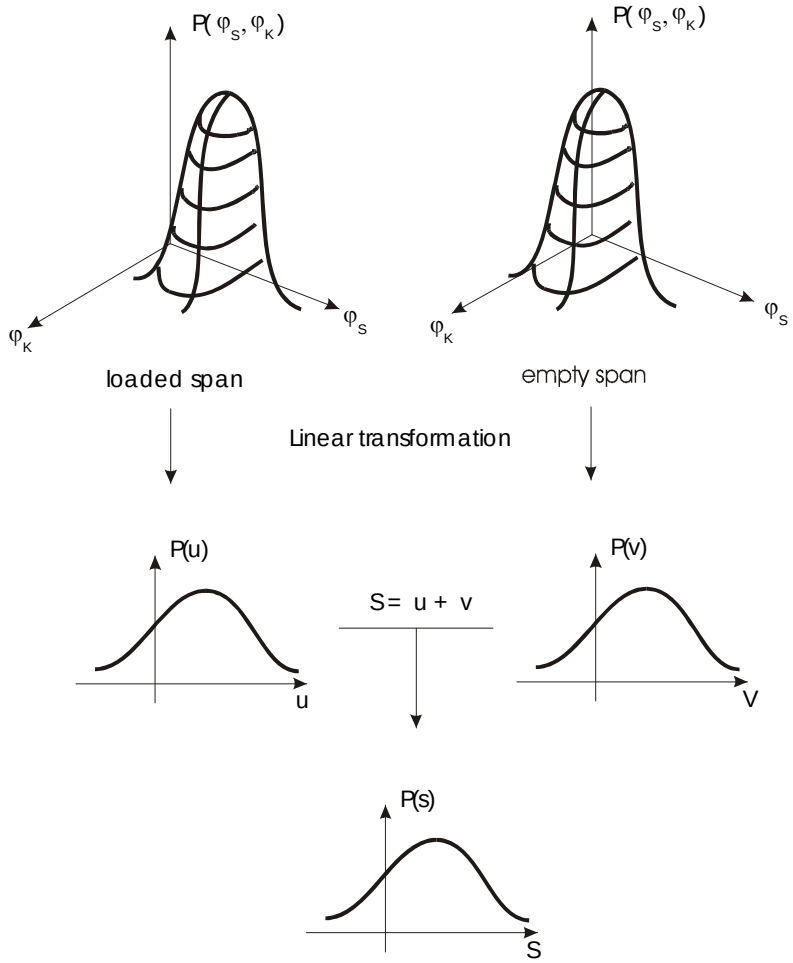

Figure 13 Schematic illustration of the calculation of the distribution density of *S*

The derivation is long and we present only its results. The distribution densities for *U* and *V* are:

$$p(u) = \frac{1}{\sqrt{2\pi} \cdot \sigma_u} e^{\frac{u^2}{2\sigma_u^2}} \tag{15}$$

and

$$p(v) = \frac{1}{\sqrt{2\pi} \cdot \sigma_v} e^{\frac{v^2}{2\sigma_v^2}} \tag{16}$$

with the variances

$$\sigma_u^2 = \sigma_2^2 \cdot l_k^2 + 2 f_1^D \cdot l_k \cdot C_{12} + f_1^{D2} \cdot \sigma_1^2 \tag{17}$$

and

$$\sigma_v^2 = \sigma_2^2 \cdot l_k^2 + 2 f_1^U \cdot l_k \cdot C_{12} + f_1^{U2} \cdot \sigma_1^2 \tag{18}$$

Here the raised indices indicate the upward (U) and the downward (D) travelling sections of the carrying rope, f_i stands for the sag in midspan. The variance of the track width can now be expressed from (17) and (18) as follows:

$$\sigma_s^2 = \sigma_u^2 + \sigma_v^2 \tag{19}$$

The distribution density of the track width is

$$p(s) = \frac{1}{\sqrt{2\pi} \cdot \sigma_s} e^{\frac{(s-\bar{s})^2}{2\sigma_s^2}} \tag{20}$$

The question now is how to calculate from equation (20) the track width that is to be built. Equation (20) defines only the (small) probability that the boundary line in the configuration shown in Figure 10 will be violated, given a side wind with a median velocity $\bar{u}$. The probability of this boundary line violation can be defined (Figure 14) formally as follows:

$$W\left[S \geq S_{ausgeführt}\right] = \int_{S_{ausgef.}}^{\infty} p(s) \cdot ds \tag{21}$$

This probability of boundary line violation should be suitably defined.

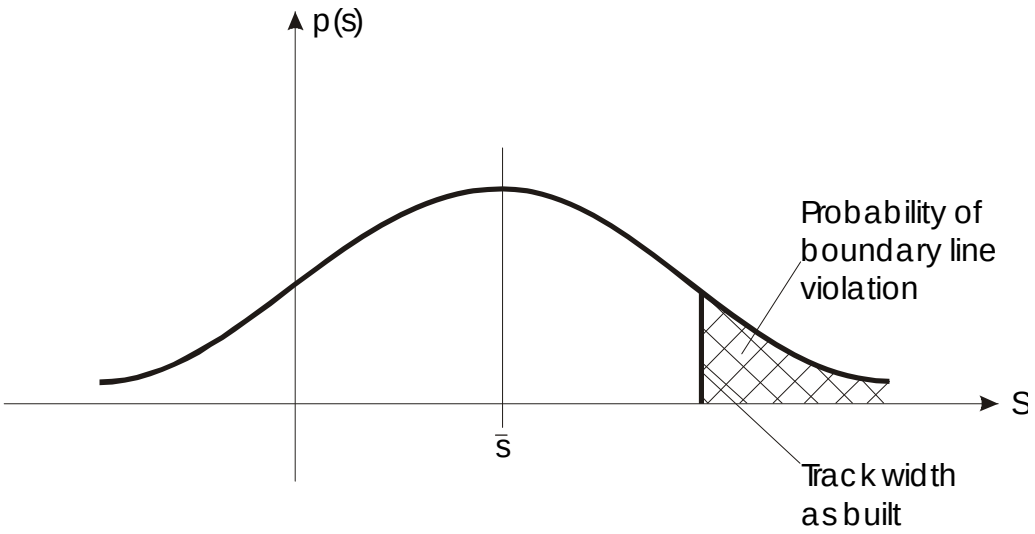

Figure 14 Distribution density of the track width.

The track width can be written from Figures 10 and 14 as

$$S = \bar{S} + S_D + B \tag{22}$$

where *B* is the cabin width, S_D is the dynamic component of the track width. The stochastic processes acting on the ropeway described in Section 2 are responsible for S_D.

The value of the probability of boundary line violation S_D is normally set based on practical experience. Empirical values used in the steel construction industry, in particular for high rise chimneys are based on

$$S_D = \gamma \cdot \sigma_S \tag{23}$$

where the value of γ is set at:

$$\gamma = 3.5 \tag{24}$$

The probability of boundary violation will then be, from (21):

$$W[S \geq \gamma \cdot \sigma_S] = 1 - \Phi(\gamma) = 0.00023 \tag{25}$$

In other words the probability of violating the boundary line shown in Figure 10 is, expressed as a percentage, 0.023%.

Using equations (22) and (23) we can write the track width as

$$S = \bar{S} + \gamma \cdot \sigma_S + B \qquad (26)$$

The median value $\bar{S}$ may be calculated from the median wind velocity $\bar{u}$. The median track width $\bar{S}$ being the difference of the two statical displacements of both tracks, its value for equal loading of the two tracks (upward and downward) is zero ($\bar{S} = 0$). With unequal loads the value of $\bar{S}$ is usually small compared to that of S_D. For the sake of completeness, it must be mentioned that for the ropeways, where the vehicles passing towers possess transverse – swinging freedom, their track with must also be proved. The method formerly described can be applied in principle. Thus there are no additional difficulties for the calculation of the track width on the tower.

6 Monitoring of oscillations of the rope span on the Funitel in Montana

Several values have to be assumed to calculate properly the track width of a ropeway using the calculations described above. An example is the damping in the system, a quantity whose value is not available at the design stage. Another quantity that is only uncertainly to estimate is the correlation factor *k* that is important in the calculation of the aerodynamic transfer function (equation (4)).

In the following we shall describe the procedure of carrying out measurements on an existing installation and estimating the missing values of parameters so that they can be used in the calculation of new installations of a similar design. The installation chosen was a Funitel one in Montana (Switzerland). This was equipped with instruments to measure the wind velocity and the sideways displacement of the rope span.

The Funitel in Montana has two fields with extreme length of span of about 1.2 km each. It is therefore particularly suited for monitoring the pendulum oscillation of these rope spans. The span nearer the lower terminal was chosen for the measurements, because both the supply of power to the measuring instrument and the signal transmission from it is easier from there.

The following measuring concept was employed:

- The rotating cup anemometer (anemograph) installed permanently on no. 2 tower are used for recording the wind velocity on the rope span.

- A video camera is installed on no. 2 tower to observe the rope span. When the wind velocity is high enough the camera switches on in single frame mode to provide three images per second of the span.

- Both the data from the anemometer and the video images are transmitted through a glass fiber link to the lower terminal and stored in a personal computer. This computer is connected through an ISDN link with another personal computer at the Swiss Federal Institute of

Technology (ETHZ) in Zürich. Here the stored data and images can be called up for evaluation.

The measuring system is shown schematically in Figure 15

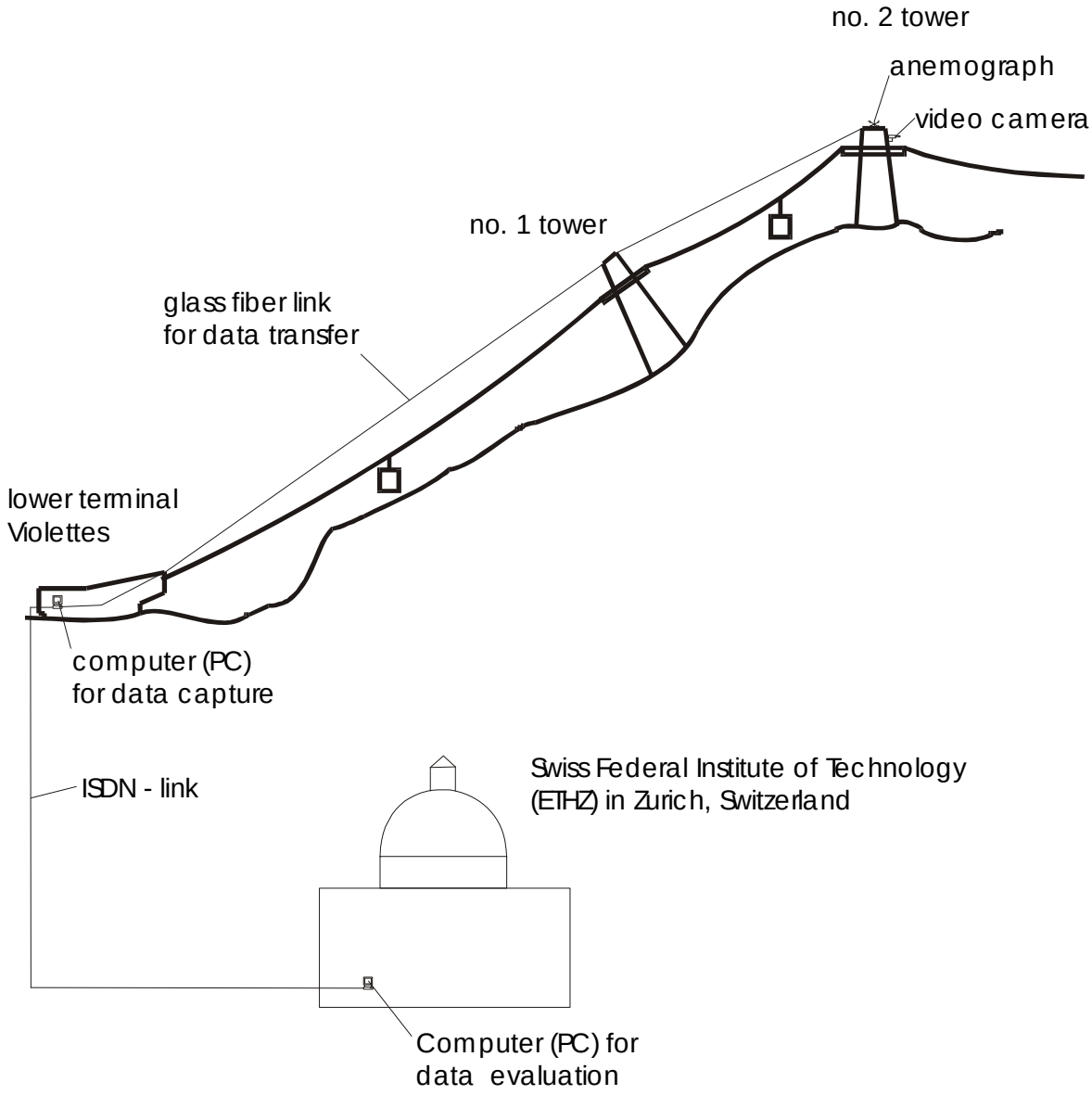

Figure 15. Measuring set-up at Funitel in Montana

The images from the video camera are annotated in the computer in Montana for data capture with the current time and date and the momentary value of wind velocity. Each image can be identified with the time of day and wind velocity. The information gives the values for the parameters in the equations of Section 2 describing rope movement. The sideways displacement of the tracks can be read from the video images. Applying a Fourier transformation to the time function of the wind velocity and to the rope

displacement gives according to equation (27), a way of describing the whole system free of parameters.

$$S_{\varphi\varphi}(f) = S_{uu}(f) \cdot |A(f)|^2 |G(f)|^2 \qquad (27)$$

from the anemometer

estimate of parameter

Estimate of system damping

From image of the video camera

The measurements are currently running. Therefore there are no definite results yet. Figure 16 is a typical image from the video camera.

Figure 16 Image from the video camera mounted on no. 2 tower of the Funitel in Montana

The system parameters of the installation from this test set-up may be used in the design of an installation of the same type. For the design of other types of installation

such as jig-back tramways and continuously circulating monocables the measurements should be repeated on a corresponding type of installation.

It should be possible to design the track width of "Funitel" type installations in the future on a scientific basis, using the procedure described in this paper.

7. Bibliography

[1] Ruscheweyh H.
Dynamische Windwirkung an Bauwerken (2 Bände)
Bauverlag GmbH Wiesbaden und Berlin 1982

[2] Prof. H. Bühlmann
Wahrscheinlichkeitsrechnung und Statistik
AMIV – Verlag 1982

[3] Zursanski J.A.
Windeinflüsse auf Baukonstruktionen
Verlagsgesellschaft Rudolf Müller Köln – Braunsfeld 1981

[4] Vickery B.J., Kao K.H.
Drag or Longwind Response of Slender Struktures
Jorn. Of the Struct. Div. Proc ASCE Vol. 93

[5] Galemann T. Ruscheweyh H.
Untersuchung winderregter Schwingungen an Stahlschornsteinen
Forschungsbericht 163
Studiengesellschaft Stahlanwendung e.V. Düsseldorf 1992

[6] Schlitt H.
Systemtheorie für regelose Vorgänge
Springer Verlag 1960

[7] Rotta J.C.
Turbulente Strömungen
B.G. Teubner Stuttgart